An Active Ball Handling Mechanism for RoboCup

Jeroen de Best and René van de Molengraft
Department of Mechanical Engineering
Eindhoven University of Technology
Eindhoven, The Netherlands
j.j.t.h.d.best@tue.nl and m.j.g.v.d.molengraft@tue.nl

***Abstract*—This paper describes a new active ball handling method for the RoboCup mid-size league as used by team Tech United at Eindhoven University of Technology. A theoretical model is derived followed by the control design including a feedback controller and a feedforward controller. The proposed control design is validated with the Tech United soccer robots. The results of several tests show the effectiveness of the new ball handling design.**

***Index Terms*—Robotics, RoboCup, Real-time control**

I. Introduction

RoboCup [4] is a worldwide competition in which autonomous robots play soccer against each other, with the ultimate goal of beating the human world champion team in 2050. There are different leagues, including the small-size league, the mid-size league and humanoid league. In the latter, robots should walk as opposed to the small-size and mid-size league where they are wheeled. This article presents a new ball handling approach for the mid-size league. In the mid-size as well as in the small-size league it is crucial to have a good ball handling during dribbling motion in order to maneuver fast through the defence of the opponents. Several methods for ball manipulation have been reported, e.g. [8], [2]. Many of the methods rely on passive systems in which the ball handling problem is shifted to a trajectory planning problem. In such systems a force can only be exerted on the ball with a component pointing away from the robot. To slow down the ball the robot has to rotate 180 degrees around the vertical axis of the ball, which constraint is included in the trajectory planning. The other type of existing methods use active open-loop mechanisms in which wheels or rollers spin backward in order to retract the ball, i.e. towards the robot [2]. However, due to small variations in the field the ball is prone to spinning backward or lying still during a forward movement, which is against the prescribed rules and regulations. Regarding ball manipulation the rules and regulations of the middle size RoboCup league [5] state that:

- The convex hull of the robot may enclose the ball only for one third of the ball diameter. During catching of the ball it may enclose half the diameter of the ball.
- The ball should rotate in its natural direction of rotation.

Obviously, the goal is to catch the ball and keep it during a dribbling motion of the robot while satisfying the rules mentioned above. This article describes a new approach in ball manipulation that is implemented in the soccer robots of the mid-size team Tech United [9]. The presented active ball handling mechanism is closed-loop in a sense that it control the distance between the ball and the robot and is superior to the commonly used ones for multiple reasons. First of all, it creates the opportunity to drive *backwards* while still possessing the ball. Secondly, the position of the ball with respect to the robot can be controlled within the range of the ball handling mechanism. This property can be exploited during a kick, where the ball can be pulled against the kicker or can be placed to the left or to the right of the kicker, which enables the robot to aim during a shot, without rotating the robot itself. Furthermore, during a dribble the ball will rotate in its natural direction at all times, independent of the texture of the field. Finally, the trajectory planning problem becomes much simpler since it not necessary to rotate around the vertical axis of the robot in order to change the direction during a dribbling motion.

The rest of this paper is organized as follows. In Section II an elementary theoretical model will be derived. This model is then used for the control design as discussed in Section III. The proposed control algorithm is implemented on the experimental setup as discussed in Section IV. The implementation of the proposed control algorithm will be given in Section V. The results of several tests that show the effectiveness of the control design will be given in Section VI. Finally, in the last section conclusions will be drawn and recommendations will be given.

II. Theoretical Model

This section describes the theoretical model for the ball handling mechanism. The 2-dimensional simplified model of the ball handling mechanism is schematically depicted in Fig. 1. In this figure, the cart represents the soccer robot. On the robot a lever is mounted that can freely rotate around a fixed point of the robot by means of a hinge. The height of this point is located at a distance h above the center of the ball as can be seen in Fig. 1. The lever has a length l, a mass m_l and a rotational inertia J_l. At the end of the lever a wheel with mass m_w and rotational inertia J_w is mounted. The radius of the wheel is denoted by R_w. A torque T can be applied between the wheel and the lever by means of a motor to control the angle of the lever and to counteract the viscous damping d that is present between the lever and the wheel. During dribbling the wheel is assumed to be in contact with the ball at all times. The ball has a radius R_b, a mass m_b and a rotational inertia J_b. Furthermore, it is assumed that

978–1–4244–2287–6/08/$25.00

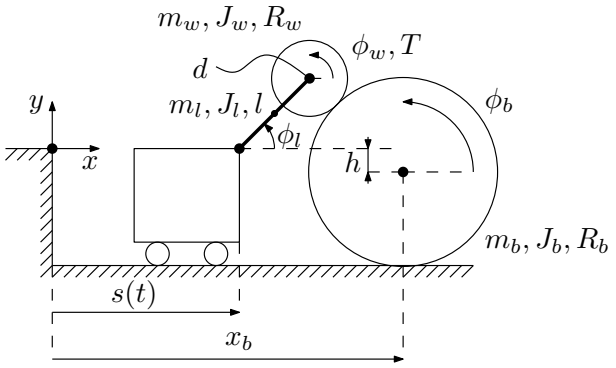

Fig. 1. The active ball handling mechanism

there is no slip between wheel and ball nor between ball and floor. The motion of the robot is prescribed and is denoted by $s(t)$. The idea is to measure the angle of the lever ϕ_l and maintain this angle at a preferred angle, which corresponds with a desired distance between the ball and the robot. In the remainder of this paper it will be shown that this can be realized by a feedback controller. The basic idea here is to apply a clockwise torque to retract the ball if the ball is too far away from the robot and to apply a counterclockwise to push the ball if it is too near.

In the remainder of this section the Lagrange's equations of motion for the system shown in Fig. 1 will be derived [6]. Therefore, the position vectors of the bodies' center of mass, i.e. $\underline{r}_l$, $\underline{r}_w$, $\underline{r}_b$ are derived as a function of the generalized coordinate ϕ_l and the prescribed coordinate $s(t)$.

$$\underline{r}_l = \begin{pmatrix} s(t) + \frac{1}{2} l \cos(\phi_l) \\ \frac{1}{2} l \sin(\phi_l) \end{pmatrix}, \tag{1}$$

$$\underline{r}_w = \begin{pmatrix} s(t) + l \cos(\phi_l) \\ l \sin(\phi_l) \end{pmatrix}, \tag{2}$$

$$\underline{r}_b = \begin{pmatrix} s(t) + l \cos(\phi_l) + \sqrt{(R_b + R_w)^2 - (l \sin(\phi_l) + h)^2} \\ -h \end{pmatrix}. \tag{3}$$

Moreover, the rotation of each body, i.e. $\underline{\theta}_l$, $\underline{\theta}_w$, $\underline{\theta}_b$ can be calculated as a function of the generalized coordinate ϕ_l and the prescribed coordinate $s(t)$.

$$\underline{\theta}_l = \phi_l, \tag{4}$$

$$\underline{\theta}_w = \frac{s(t) + l \cos(\phi_l) + \sqrt{(R_b + R_w)^2 - (l \sin(\phi_l) + h)^2}}{R_w} - \frac{\arcsin\left(\frac{l \sin \phi_l + h}{R_b + R_w}\right)}{R_w}, \tag{5}$$

$$\underline{\theta}_b = \frac{s(t) + l \cos(\phi_l) + \sqrt{(R_b + R_w)^2 - (l \sin(\phi_l) + h)^2}}{R_b}. \tag{6}$$

The velocity vectors of the bodies can be calculated as

$$\underline{v}_l = \frac{d\underline{r}_l}{d\phi_l}\frac{d\phi_l}{dt} + \frac{d\underline{r}_l}{ds}\frac{ds}{dt} = \frac{d\underline{r}_l}{d\phi_l}\dot{\phi}_l + \frac{d\underline{r}_l}{ds}\dot{s}, \tag{7}$$

$$\underline{v}_w = \frac{d\underline{r}_w}{d\phi_l}\frac{d\phi_l}{dt} + \frac{d\underline{r}_w}{ds}\frac{ds}{dt} = \frac{d\underline{r}_w}{d\phi_l}\dot{\phi}_l + \frac{d\underline{r}_w}{ds}\dot{s}, \tag{8}$$

$$\underline{v}_b = \frac{d\underline{r}_b}{d\phi_l}\frac{d\phi_l}{dt} + \frac{d\underline{r}_b}{ds}\frac{ds}{dt} = \frac{d\underline{r}_b}{d\phi_l}\dot{\phi}_l + \frac{d\underline{r}_b}{ds}\dot{s}. \tag{9}$$

The rotational velocities can be calculated similarly

$$\underline{\omega}_l = \frac{d\underline{\theta}_l}{d\phi_l}\frac{d\phi_l}{dt} + \frac{d\underline{\theta}_l}{ds}\frac{ds}{dt} = \frac{d\underline{\theta}_l}{d\phi_l}\dot{\phi}_l + \frac{d\underline{\theta}_l}{ds}\dot{s}, \tag{10}$$

$$\underline{\omega}_w = \frac{d\underline{\theta}_w}{d\phi_l}\frac{d\phi_l}{dt} + \frac{d\underline{\theta}_w}{ds}\frac{ds}{dt} = \frac{d\underline{\theta}_w}{d\phi_l}\dot{\phi}_l + \frac{d\underline{\theta}_w}{ds}\dot{s}, \tag{11}$$

$$\underline{\omega}_b = \frac{d\underline{\theta}_b}{d\phi_l}\frac{d\phi_l}{dt} + \frac{d\underline{\theta}_b}{ds}\frac{ds}{dt} = \frac{d\underline{\theta}_b}{d\phi_l}\dot{\phi}_l + \frac{d\underline{\theta}_b}{ds}\dot{s}. \tag{12}$$

With these results the kinetic energy of the system becomes

$$K = \sum_{i \in \{l,w,b\}} \frac{1}{2} m_i \underline{v}_i^T \underline{v}_i + \frac{1}{2} J_i \underline{\omega}_i^T \underline{\omega}_i. \tag{13}$$

The potential energy can be written as

$$V = \frac{1}{2} m_l g l \sin(\phi_l) + m_w g l \sin(\phi_l) - m_b g h, \tag{14}$$

where g is the gravity constant.
With (13) and (14) the Lagrange's equations of motion can be calculated as

$$\frac{d}{dt}\left(\frac{dK}{d\dot{\phi}_l}\right) - \frac{dK}{d\phi_l} + \frac{dV}{d\phi_l} = Q_{nc}^T, \tag{15}$$

where Q_{nc} are the non-conservative forces. These forces consist of the applied torque T and the torque caused by the damping d between the lever and the wheel modeled as $T_d = d(\dot{\phi}_w - \dot{\phi}_l)$. These non-conservative forces are formulated as

$$Q_{nc} = \left(\frac{d\underline{\theta}_w}{d\phi_l} - \frac{d\underline{\theta}_l}{\phi_l}\right)(T_d - T). \tag{16}$$

Finally, a non-linear model can be constructed which has the form

$$\ddot{\phi}_l = f(\phi_l, \dot{\phi}_l, \dot{s}(t), \ddot{s}(t), T). \tag{17}$$

III. Control Design

Figure 1 shows a typical point of operation. Intuitively, one can see that such a point of operation is unstable. If there is no actuation, the lever will simply drop down due to gravity forces. In order to stabilize these operation points a feedback controller will be constructed based on a linearized model derived from (17). To further improve the tracking performance of the system, a feedforward controller will be designed as discussed in Section III-B.

A. Feedback Design

In the previous section the non-linear model of the ball handling mechanism was derived. This section presents the design of a stabilizing feedback controller. For the design of the feedback controller the non-linear model is linearized around the following desired equilibrium point

$$\phi_{l,eq} = \frac{\pi}{4},\ \dot{\phi}_{l,eq} = 0,\ \dot{s}_{eq} = 0,\ \ddot{s}_{eq} = 0,\ T_{eq}. \tag{18}$$

In the choice of this equilibrium point it is checked whether or not the chosen equilibrium point satisfies the preferred distance between the ball and the robot. Other equilibrium points may be chosen as well, since this does not influence the presented control method. The torque T_{eq}, associated with the chosen equilibrium point, can be calculated by substituting the values of (18) into (17) and solving for T_{eq} from

$$0 = f(\phi_{l,eq}\dot{\phi}_{l,eq}, \dot{s}_{eq}, \ddot{s}_{eq}, T_{eq}). \tag{19}$$

Linearization around the point of operating results in the following second order linear model

$$G : \left\{ \begin{array}{rcl} \dot{\underline{x}} & = & A\underline{x} + Bu \\ y & = & C\underline{x} + Du \end{array} \right. , \tag{20}$$

where the state vector is given by $\underline{x} = \begin{bmatrix} \phi_l - \phi_{l,eq} & \dot{\phi}_l \end{bmatrix}^T$, the input u is given by $T - T_{eq}$ and the output y is defined as $\phi_l - \phi_{l,eq}$. The system matrix A, input matrix B and output matrix C are given by

$$A = \begin{bmatrix} 0 & 1 \\ \frac{df}{d\phi_l} & \frac{df}{d\dot{\phi}_l} \end{bmatrix}, B = \begin{bmatrix} 0 \\ \frac{df}{dT} \end{bmatrix}, C = \begin{bmatrix} 1 & 0 \end{bmatrix}, D = \begin{bmatrix} 0 \end{bmatrix}, \tag{21}$$

where A and B are both evaluated at the equilibrium point (18).
Using the linearized model (20) single-input single-output control techniques can be applied in order to tune a feedback controller $\mathcal{K}$ that stabilizes the equilibrium point. The results of the proposed feedback controller will be given in Section VI.

B. Feedforward Design

In the previous section the operation point was chosen such that the acceleration of the robot is zero. In practice this will not be the case, since the robot will almost constantly move during a game. This brings us to the design of a feedforward controller, where we linearize the non-linear model around

$$\phi_{l,eq} = \frac{\pi}{4},\ \dot{\phi}_{l,eq} = 0,\ \dot{s}_{eq} = \dot{s}(t),\ \ddot{s}_{eq} = \ddot{s}(t),\ T_{eq}, \tag{22}$$

such that the torque T_{eq} will be a function of the velocity and acceleration of the robot, i.e. $T_{eq}(\dot{s}(t), \ddot{s}(t))$. Since the velocity $\dot{s}(t)$ and acceleration $\ddot{s}(t)$ are known we can calculate the torque T_{eq} and use it as a feedforward input in the control scheme to improve the tracking performance of the considered system. The total control scheme is schematically given in Fig. 2. The improvements will be shown in Section VI.

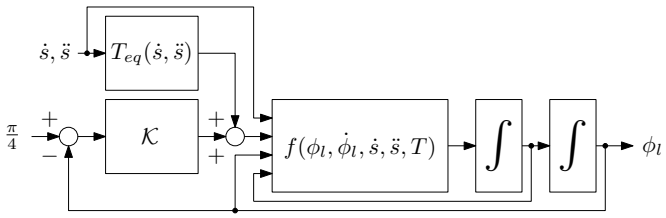

Fig. 2. The control scheme.

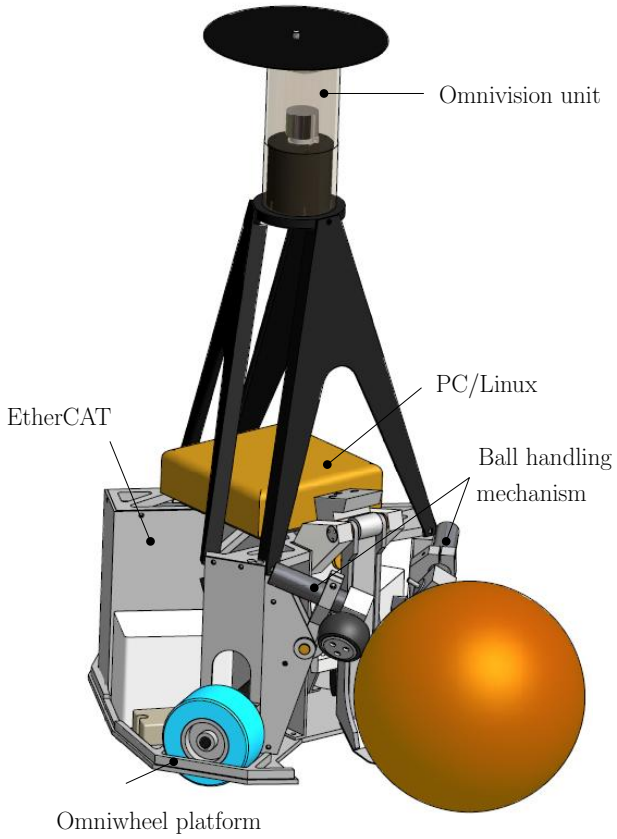

Fig. 3. The soccer robot.

IV. Experimental Setup

This section describes the experimental setup that is used to implement the proposed control algorithm in practice. The setup is schematically depicted in Fig. 3. The robot is driven by three omniwheels. Each omniwheel is driven by a separate Maxon RE40 150W DC motor. To be able to kick, a solenoid is designed [10], which delivers shooting capabilities up to approximately 10 m/s. The ball handling wheels are driven by Maxon RE25 20W DC motors, whereas the angles of the levers can be measured with potentiometers. Like many other teams, the robot is equipped with omnidirectional vision that is used for self localization and ball and obstacle detection. Beckhoff [1] EtherCAT [3] modules are used for the real-time acquisition. These modules are connected to an industrial PC running a 2.6.23.1 SMP PREEMPT Linux kernel, which runs

the control algorithms.

V. Control Algorithm Implementation

In Fig. 4 the top view of the ball handling of the soccer robot is highlighted. As can be seen from this figure the soccer robot has two levers in order to grab and handle the ball. This can be explained by the fact that such a configuration enables the opportunity to handle the ball in both the forward and sideward movements of the robot during a dribbling motion. More specifically, if a forward movement is carried out both wheels are driven such that they push the ball. During a sideward movement one of the levers is driven to retract the ball whereas the other is driven as to push the ball. This however leads to a multi-input multi-output (MIMO) system, since there are now two actuators that can influence the motion of the ball. Furthermore, there are two sensors to measure the ball position.

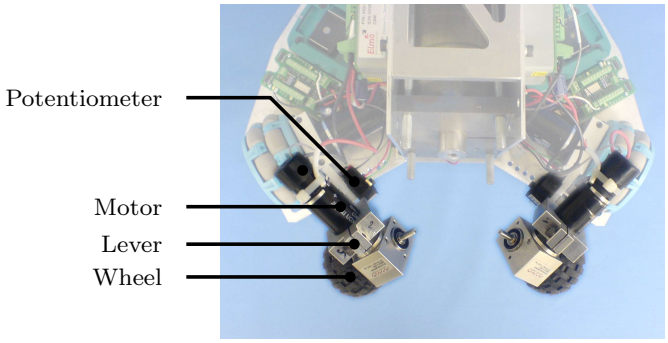

Fig. 4. Top view ball handling.

By placing the levers under an angle of 90 degrees with respect to each other as seen from the top view, the cross coupling of the multi-input multi-output system is minimized. Hence, we can still use the single-input single-output control design as described in Section III. This assumption is validated via the measured relative gain array (RGA) [7] which is shown in Fig. 5. The relative gain array provides a measure of interaction which is independent of input and output scaling. The RGA is defined as

$$\Lambda(\tilde{G}) = \tilde{G} \times (\tilde{G}^{-1})^T, \tag{23}$$

where $\tilde{G}$ is the two-input two-output plant and $\times$ denotes element-by-element multiplication (the Schur product). In order to apply decentralized control it is preferred that this matrix is close to the unity matrix I for all frequencies. From Fig. 5 it can be seen that the system can be considered to be decoupled up to approximately 10 Hz. Therefore, until 10 Hz, the system can be considered to be decoupled. For this reason, the aimed bandwidth of the feedback controller will also be less than 10 Hz.

In Section II it is was assumed that the wheels of the ball handling mechanism are in contact with the ball at all times.

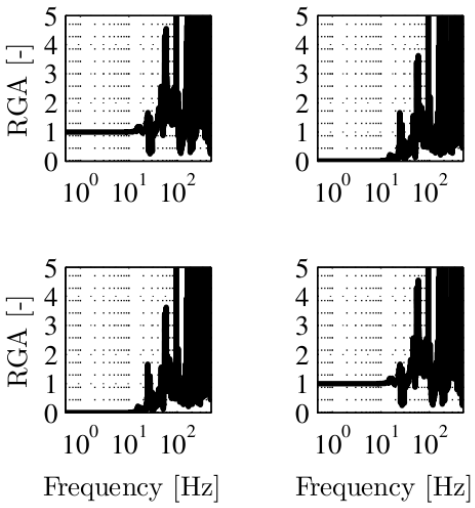

Fig. 5. The measured relative gain array.

However, this is of course not the case when the robot does not have the ball. In that case both levers are in the outer forward position which is restricted to approximately $\pi/8$ [rad]. In this position the feedback controllers still attempt to control the angle ϕ_l. However, since the dynamics of the system have changed this is impossible. The above reasoning clarifies why no integral action is implemented in the feedback controller. The integral action would result in a wind-up if the robot does not have the ball. If the robot is in possession of the ball it will would immediately spin backward which is against the rules.

VI. Results

This section describes the results obtained with the presented control design. The parameters of the experimental setup are given in Table I:

TABLE I
Parameters of the ball handling setup

Parameter	Description	Value	Unit
l	Length of the lever	0.07	[m]
m_l	Mass of the lever	0.3	[kg]
J_l	Inertia of the lever	$\frac{m_l l^2}{12}$	$[\text{kgm}^2]$
R_w	Radius of the wheel	0.028	[m]
m_w	Mass of the wheel	0.1	[kg]
J_w	Inertia of the wheel	$\frac{m_w R_w^2}{2}$	$[\text{kgm}^2]$
R_b	Radius of the ball	$\frac{0.69}{2\pi}$	[m]
m_b	Mass of the ball	0.43	[kg]
J_b	Inertia of the ball	$\frac{2m_b R_b^2}{3}$	$[\text{kgm}^2]$
d	Damping between lever and wheel	0.005	[Nmrad/s]
h	Height of rotation point of lever	0.035	[m]
g	Gravity constant	9.81	[m/s^2]

With these parameters the linearized model G becomes

$$\begin{aligned} \dot{\underline{x}} &= \begin{bmatrix} 0 & 1 \\ 21.28 & -22.45 \end{bmatrix} \underline{x} + \begin{bmatrix} 0 \\ 757.24 \end{bmatrix} u \\ y &= \begin{bmatrix} 1 & 0 \end{bmatrix} \underline{x} + \begin{bmatrix} 0 \end{bmatrix} u \end{aligned} . \quad (24)$$

The poles of this system are located at 0.91 and -23.36, which indicates that the considered system is indeed unstable.
To validate the model a frequency response function (FRF) is measured on the experimental setup. The result of one of those measured FRFs is given in Fig. 6. From this figure it can be seen that the model matches the measured frequency response measurement quite well. However, beyond 10 Hz, the measurement in not reliable any more, since above this frequency the amplitude of the angle of the lever becomes that small that it is hardly visible due to the sensor noise, which leads to a poor signal to noise ratio. Furthermore, unmodeled artifacts of the ball handling mechanism show up in the measured frequency response function. One of these artifacts might represent the finite stiffness of the tires of the ball handling wheels. Moreover, since the control algorithm is implemented in discrete time the system also inherently suffers from time delay, which is also not taken into account in the modeling of dynamics of the ball handling mechanism.

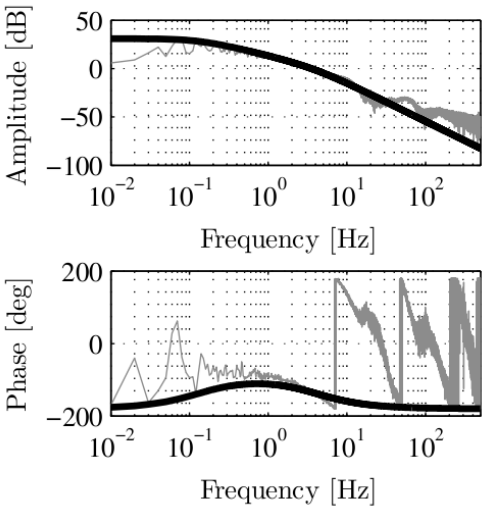

Fig. 6. Measured frequency response function (grey), linearized model (24) (black).

By using loopshaping techniques [11], a simple output feedback controller with a single proportional gain can be used to stabilize the system given in (24). This feedback controller $\mathcal{K}$ is given by

$$u = e = r - y, \quad (25)$$

with the tracking error e defined as $e = r - y$. Then, Fig. 6 can be interpreted as the open loop of the system, with a bandwidth of approximately 4 Hz. The closed loop poles are given by -11±25i, hence a stable closed loop system is obtained.

With the designed feedback controller (25) a simulation is carried out in order to demonstrate the effectiveness of the proposed control design. It is chosen to show a 1-D simulation results rather than 2-D experimental results to concentrate on the principle of operation of the control design. The angle of the lever ϕ_l is initially set to $\frac{\pi}{8}$ [rad] while the soccer robot is in stand still position, $s(t) = 0\ \forall t$. At $t = 0.5$ [s] the reference is set to $\frac{\pi}{4}$ [rad]. The results of this simulation are shown in Fig. 7 The figures on the left hand side show the responses

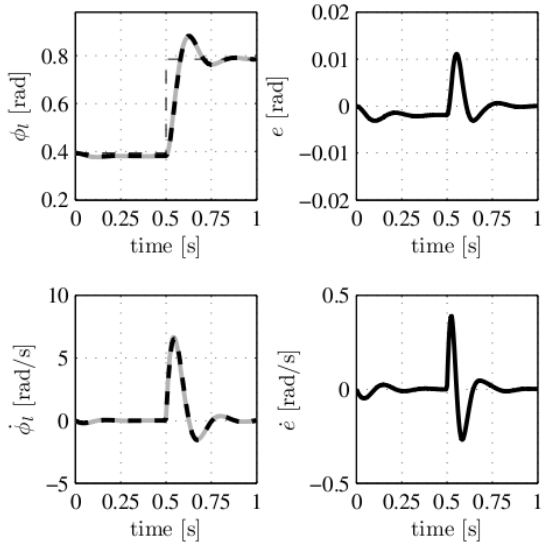

Fig. 7. Step response of the closed-loop linear and non-linear model.

of the angle ϕ_l as well as the angular velocity $\dot{\phi}_l$ for both the non-linear model, represented by a grey solid line, and the linear model, represented by a black dashed line. The figures on the right hand side reflect the differences between the non-linear model and linear model. From these figures it can be observed that the step reference results in a transient behavior at the output. The reference step is followed with an overshoot of 0.09 [rad] and a settling time of less than 0.2 sec. Furthermore, it can seen that the difference between the non-linear model and linear model is very small. This justifies the use of a linear model for the control design.

In the previous simulation the velocity of the robot was set to zero, $s(t) = 0\ \forall t$. As can be imagined, this situation is rare during a soccer game. Therefore, another simulation is carried out while the robot is accelerating, $\ddot{s}(t) \neq 0$. From these simulations, the effectiveness of the feedforward controller is shown. In order to quantify the effect of the feedforward controller two simulations are carried out, one without feed-

forward controller and one with feedforward controller. During the simulation the robot is accelerating with 0.5 [m/s^2] and at $t = 0.5$ [s] again the reference is changed from $\pi/8$ [rad] to $\pi/4$ [rad]. The results of these simulations are shown in Fig. 8. The solid line in Fig. 8 is the response of the non-

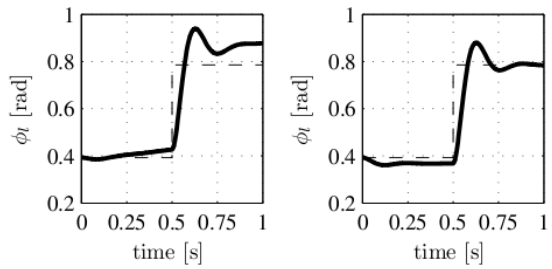

Fig. 8. Step response of the closed-loop system during acceleration without feedforward (left) and with feedforward (right).

linear model (17). On the left hand side the result without feedforward controller is shown whereas on the right hand side the result of the simulation with feedforward controller is shown. It can be observed that if no feedforward controller is applied a non-zero error remains. This error is caused by the inertial forces of the bodies which act on the lever. Furthermore, the observed error is the result of the damping force that is generated when the wheel is turning with respect to the lever. The error is reduced by implementing the feedforward controller as described in Section III-B. This feedforward is of the form

$$T_{eq}(\dot{s}(t), \ddot{s}(t)) = a_2\ddot{s}(t) + a_1\dot{s}(t) + a_0, \tag{26}$$

where the coefficients $a_i, i \in \{0, 1, 2\}$ result from (22). From the results shown in Figure 8 it can be seen that the tracking error of the reference angle vanishes due to the feedforward action.

VII. Conclusions and Recommendations

In this paper a novel approach was presented regarding the ball handling that is used in the Tech United mid-size RoboCup team. A non-linear model was formulated for the setup, which after linearization is used for the feedback control design, leading to a stable closed loop system with a bandwidth of approximately 4 Hz. To further improve the tracking performance a feedforward controller was implemented leading to a significant decrease of the tracking error of the preferred reference angle. The effectiveness of the proposed control algorithm is shown. Future research will focus on the possibilities for aiming the ball before shooting without rotating the robot itself which can be achieved by altering the reference angles of the levers. Other possibilities like kicking with the ball handling mechanism instead of the kicker now belong to the possibilities but still have to be investigated in near future.

References

[1] Beckhoff, *EtherCAT, Ultra high-speed communication*, http://www.beckhoff.de/english.asp?ethercat/default.htm, 2008

[2] R. D'Andrea, T. Kalmar-Nagy, P. Ganguly, M. Babish, *The Cornell RoboCup Team* in RoboCup 2000: Robot Soccer World Cup IV, P.Stone, T. Balch and G. Kraetzschmar, Eds., NewYork: Springer, (2002), pp. 41-51.

[3] D. Janssen, H. Buttner, *Real-time ethernet the EtherCAT solution*, Computing and Control Engineering Journal, vol 15, no 1, 2004

[4] RoboCup, RoboCup Official site, www.robocup.org

[5] MSL Technical Committee 1997-2008, *Middle Size Robot League Rules and Reglations for 2008*, draft version 12.2 20071109. (2007)

[6] A. de Kraker, D.H. van Campen, *Mechanical Vibrations*, Shaker Publishing BV, ISBN 90-423-0165-1 (2001)

[7] S. Skogestadt and I. Postlethwaite, *Multivariable Feedback Control, Analysis and Design (2nd Edition)*, Wile, ISBN 13-978-0-470-01168-3 (2007)

[8] S. Stancliff, *Evolution of Active Dribbling Mechanisms in RoboCup*, 16-471 Project, April (2005)

[9] Tech United. Technische Universiteit Eindhoven: Tech United. http://www.techunited. nl, 2008.

[10] R. Tilburgs, *Design and realization of a solenoid for a Robocup kicking device*, 22, DCT 2006.120, Internal Report, Technische Universiteit Eindhoven. (2006)

[11] G.F. Franklinn, J.D Powell, A Enami-Naeihi, *Feedback Control of Dynamic Systems*, Addison-Wesley Publishing Company, ISBN 0-201-52747-2, (1994)